IEEE Access
Multidisciplinary | Rapid Review | Open Access Journal

Received May 2, 2019, accepted May 28, 2019, date of publication June 5, 2019, date of current version June 20, 2019.

Digital Object Identifier 10.1109/ACCESS.2019.2920916

Implementation of Univariate Paradigm for Streamflow Simulation Using Hybrid Data-Driven Model: Case Study in Tropical Region

ZAHER MUNDHER YASEEN[1], WAN HANNA MELINI WAN MOHTAR[2], AMEEN MOHAMMED SALIH AMEEN[3], ISA EBTEHAJ[4], SITI FATIN MOHD RAZALI[2], HOSSEIN BONAKDARI[4], SINAN Q SALIH[5,6], NADHIR AL-ANSARI[7], AND SHAMSUDDIN SHAHID[1]

[1]School of Civil Engineering, Faculty of Engineering, Universiti Teknologi Malaysia, Skudai, Johor Bahru 81310, Malaysia
[2]Sustainable and Smart Township Research Centre (SUTRA), Faculty of Engineering and Built Environment, Universiti Kebangsaan Malaysia, Bangi, Selangor 43600, Malaysia
[3]Department of Water Resources, University of Baghdad, Baghdad, Iraq
[4]Department of Civil Engineering, Razi University, Kermanshah 97146, Iran
[5]Institute of Research and Development, Duy Tan University, Da Nang 550000, Vietnam
[6]Computer Science Department, College of Computer Science and Information Technology, University of Anbar, Ramadi, Iraq
[7]Civil, Environmental and Natural Resources Engineering, Lulea University of Technology, 97187 Lulea, Sweden

Corresponding author: Zaher Mundher Yaseen (myzaher@utm.my)

This work was supported by the Professional Development Research University (PDRU) under Grant Q.J130000.21A2.04E47.

ABSTRACT The performance of the bio-inspired adaptive neuro-fuzzy inference system (ANFIS) models are proposed for forecasting highly non-linear streamflow of Pahang River, located in a tropical climatic region of Peninsular Malaysia. Three different bio-inspired optimization algorithms namely particle swarm optimization (PSO), genetic algorithm (GA), and differential evolution (DE) were individually used to tune the membership function of ANFIS model in order to improve the capability of streamflow forecasting. Different combination of antecedent streamflow was used to develop the forecasting models. The performance of the models was evaluated using a number of metrics including mean absolute error (MAE), root mean square error (RMSE), coefficient of determination (R^2), and Willmott's Index (WI) statistics. The results revealed that increasing number of inputs has a positive impact on the forecasting ability of both ANFIS and hybrid ANFIS models. The comparison of the performance of three optimization methods indicated PSO improved the capability of ANFIS model (RMSE = 7.96; MAE = 2.34; R^2 = 0.998 and WI = 0.994) more compared to GA and DE in forecasting streamflow. The uncertainty band of ANFIS-PSO forecast was also found the lowest (±0.217), which indicates that ANFIS-PSO model can be used for reliable forecasting of highly stochastic river flow in tropical environment.

INDEX TERMS Streamflow forecasting, fuzzy logic, evolutionary algorithm, uncertainty analysis, tropical environment.

I. INTRODUCTION

Streamflow forecasting is one of the essential concerns for hydrologists and engineers for the planning and management of water resources and for designing water resources projects. Short-term and long-term streamflow forecasting can provide a valuable information on the possibility of designing and managing water infrastructures and the availability of water resources [1]–[3]. Therefore, a wide variety of methods has been developed and successfully implemented for forecasting river flow. Streamflow forecasting can be categorized into four categories: conceptual, metric, physical-based, and data-driven models [4]. Conceptual models evaluate hydrological processes i.e. precipitation, water storage, evaporation, rainfall runoff, evapotranspiration using simple equations. However, the major drawback of these models is the difficulties

The associate editor coordinating the review of this manuscript and approving it for publication was Mauro Tucci.

in calibration of the results due to involvement of many variables in the equation [5]. Metric models use the gathered hydrological data such as rainfall as its basic input. While the physical-based models employ water-balance equations based on the law of energy conservation for modelling streamflow. Lastly, the data-driven models establish relationship between input and output variables for forecasting streamflow. The data-driven models do not need catchment physical information and able to forecast streamflow with limited amount and incomplete data [5]. Therefore, such models have been widely used for forecasting streamflow in recent years.

Linear regression is traditionally used for the development of data-driven models. The capability of linear regression-based models is very limited to forecast non-linear pattern of streamflow. To overcome this difficulty, data-driven models based on soft computing (SC) techniques have been vastly developed in last three decades [5]–[9]. In recent years, there has been massive attention of exploring and developing new innovative SC methods that can mimic and capture highly complicated streamflow pattern [10]. This is owing to their feasibility on capturing the complexity of stochastic problems such as nonlinearity, nonstationary and redundancy [11]. A large number of data-driven models using SC techniques such as artificial neural network (ANN), fuzzy logic, adaptive network-based fussy interface system, genetic programming, and swarm intelligence methods have been proposed for forecasting streamflow [12]. However, the forecasting ability of the models in terms of accuracies are often debatable [13], [14]. This is because of the non-linear pattern of streamflow which limits the ability of the aforementioned models.

The ANN is the most popular SC-based method employed for streamflow forecasting due its capability to solve diverse complex problems [15]–[17]. The assignment of weights to the neurons for optimum performance of ANN is the major challenge in ANN-based forecasting model. The weights are controlled by both the internal tuning parameters of network learning algorithm and its architecture. In addition, the use of multiple layers with many nodes as hidden layer results an extremely complex system. The learning rates and the number of memory taps also significantly impact the performance of ANN model.

Besides ANN, the fuzzy logic (FL) which uses the concept of uncertainty is another SC-based technique that has been received much attention for modeling hydrological phenomena in last three decades [18], [19]. Similar to ANN, the FL has several shortcomings such as decision on suitable variables. To overcome the drawbacks of ANN and FL, adaptive neuro-fuzzy inference system (ANFIS) which is a combination of ANN and FL is introduced. ANFIS is a class of adaptive multi-layer feedforward networks that use fuzzy logic in performing different functions or criteria for better outcomes and intelligence [20]. It utilizes parallel computation where the learning ability is obtained from ANN and the problem-solving ability based on if-then rules is gained from fuzzy logic. Therefore, the advantages of ANN and FL can be utilized in ANFIS while the shortcomings of the individual methods can be overcome at the same time. ANFIS can fulfill approximation function and follow rules efficiently almost similar to human intuition [21] and thus, leads to higher accuracy in prediction [22]. The implementation of neuro-fuzzy concept can positively solve the non-linear characteristics and the associated uncertainties [23].

The major algorithms used for training ANFIS are back-propagation (BP), hybrid of BP and least square (BP-LS). A number of studies have been conducted to evaluate the performance of the training algorithms to determine the best ANFIS model for streamflow forecasting [24], [25]. The most remarkable shortcomings of these algorithms are trapping in the local optima during the learning process and very slow convergence [26], [27]. Newly developed intelligence algorithms such as nature inspired algorithms like particle swarm optimization, genetic algorithm, differential evolution etc. have been used in the recent years for the optimization of ANFIS parameters to improve its forecasting ability [28], [29]. The integration of evolutionary optimization algorithms with artificial intelligence (AI) models has showed outstanding performance in regression problems [30]–[33]. Thus, research focusing on identification of best optimization algorithm to be used with AI in order to achieve the most accurate and effective streamflow forecasting has gained much attention in recent years. PSO, GA and DE algorithms have been found to optimize ANFIS model effectively where the local minima and dimension problems are positively solved [34].

The main objective of the present study is to explore the feasibility of newly developed robust hybridized intelligence models, ANFIS integrated with three optimization algorithms, i.e. particle swarm optimization (ANFIS-PSO), genetic algorithm (ANFIS-GA) and differential evolution algorithm (ANFIS-DE) for forecasting monthly streamflow based on univariate modeling paradigm where only the antecedent streamflow data is used to build the predictive model. The performance of such hybrid models in forecasting streamflow in tropical environment has not been investigated yet. The models developed in the present study were used for forecasting highly stochastic streamflow of Pahang River located in the central region of Peninsular Malaysia. The streamflow of Pahang River is influenced by highly variable rainfall dominated by two monsoons. Besides, the heavy convective rainfall during inter-monsoonal periods has made the streamflow of the river highly complex. The Pahang River, the longest river in Peninsular Malaysia often experiences floods due to extreme rainfall during northwest monsoon (November-March). Reliable forecasting of streamflow of Pahang River is therefore very important for Malaysia.

II. CASE STUDY

The Pahang River lies between the latitude 2°48′45″ - 3°40′24″N and longitude 101°16′31″ - 103°29′34″E (Figure 1). The total length of the river is 460 km which

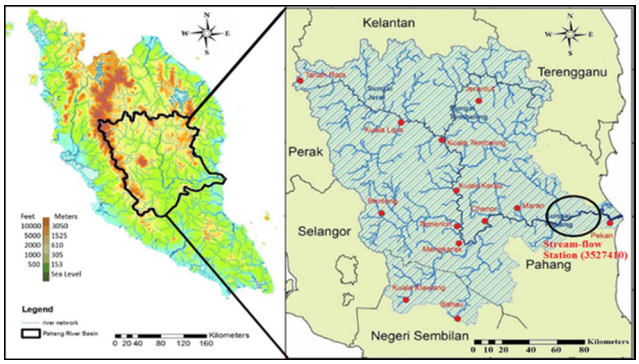

FIGURE 1. Location of Pahang River in the map of Peninsular Malaysia.

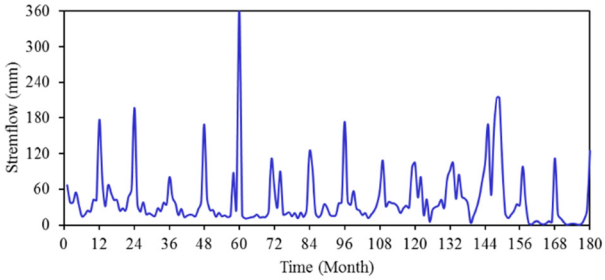

FIGURE 2. Streamflow time series of Pahang River at a station 3527410.

covers a catchment area of approximately 27,000 km^2. The streamflow of Pahang River is highly variable and stochastic [35]. This is owing to the fact that the climate of the catchment is characterized by high monsoon rainfall which causes a high fluctuation in the flow. The motivation of the development of an intelligent forecasting system for this specific river lies on the necessity of flood forecasting and estimation of water availability. The streamflow of Pahang river measured at a station (ID 3527410), located in the most downstream (Lubok Paku) of the river was used in the present study. Monthly streamflow data for the period 2000-2014 was collected from the Department of Irrigation and Drainage (DID), Malaysia. Flood is a common phenomenon in Pahang River basin. It experienced 18 major floods during 2006-2014 which caused extensive damage to properties and inconvenience to the local community. In December 2007, a large flood in Pahang River basin caused an inundation depth of about 2.0 m in Pekan and some other major towns of Termerloh and Maran districts [36]. About US$ 86 Million was estimated as the total flood damage. Forecasting river flow at monthly scale can indicate the possibility of occurrence of floods which in turn can help in flood management and mitigation of its impacts on society and economy. The streamflow time series of Pahang River is presented in Figure 2.

III. METHODOLOGY

A. ANFIS MODELLING THEORY

The main concept of neuro-fuzzy system is a modeling framework to overcome the impediments in both neural network and fuzzy logic [37]. Therefore, ANFIS has been found well

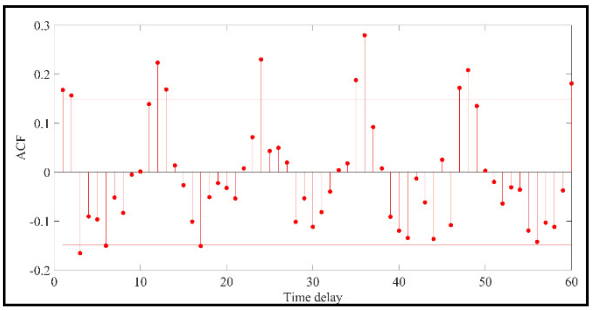

FIGURE 3. Auto-correlation function (ACF) of the raw streamflow time series.

TABLE 1. Different input combinations of antecedent data considered for the development of streamflow forecasting models.

Model Designation	Input combination(s)
M1	$t-1$
M2	$t-1, t-2$
M3	$t-1, t-3$
M4	$t-1, t-6$
M5	$t-1, t-12$
M6	$t-1, t-2, t-3$
M7	$t-1, t-2, t-6$
M8	$t-1, t-2, t-12$
M9	$t-1, t-3, t-6$
M10	$t-1, t-3, t-12$
M11	$t-1, t-2, t-3, t-6$
M12	$t-1, t-2, t-3, t-12$
M13	$t-1, t-2, t-6, t-12$
M14	$t-1, t-2, t-3, t-6, t-12$

TABLE 2. The initial values of the GA, DE and PSO optimization algorithms used in the present study.

Method	Variable	Value
All	Iteration number	1000
	Population size	150
DE	Mutation factor (F)	0.2
	crossover operator (CR)	0.75
GA	Crossover Percentage	0.7
	Mutation Percentage	0.15
PSO	C_1	2
	C_2	2

suited for identification of nonlinearity and non-stationary in time series [12]. The membership functions (MFs) of ANFIS network is tuned using ANN [38] which incorporate nonlinear MFs and subsequently result in considerable lessening in implementation cost. Predominantly, Takagi-Sugeno-Kang fuzzy inference system (FIS) is used in ANFIS, owing to its simplicity and requirement of less rules for model training. The details of ANFIS can be found in [38].

B. PARTICLE SWARM OPTIMIZATION (PSO)

The PSO is an evolutionary population-based optimization algorithm. In PSO optimization algorithm, the particles' position is changed through the optimization process in a defined multi-dimensional exploration area so that each

TABLE 3. Statistical performance of ANFIS, ANFIS-DE, ANFIS-GA, and ANFIS-PSO models for different input combinations estimated using RMSE, MAE, R2, and WI during training phase.

	RMSE (m^3/s)				MAE (m^3/s)				R^2				WI			
	ANFIS	ANFIS-DE	ANFIS-GA	ANFIS-PSO	ANFIS	ANFIS-DE	ANFIS-GA	ANFIS-PSO	ANFIS	ANFIS-DE	ANFIS-GA	ANFIS-PSO	ANFIS	ANFIS-DE	ANFIS-GA	ANFIS-PSO
M1	42.13	43.81	28.90	40.43	22.56	23.14	17.72	21.04	0.227	0.164	0.644	0.292	0.574	0.485	0.867	0.618
M2	26.98	24.88	25.07	22.01	17.12	15.52	15.80	12.77	0.686	0.733	0.729	0.791	0.892	0.913	0.911	0.935
M3	29.31	29.81	31.25	25.85	17.29	14.11	15.26	13.70	0.626	0.614	0.575	0.710	0.870	0.862	0.844	0.906
M4	33.65	32.67	34.24	32.49	18.00	16.05	16.54	15.37	0.507	0.534	0.488	0.539	0.799	0.820	0.789	0.826
M5	26.17	16.00	14.72	15.38	12.33	9.85	9.41	8.64	0.697	0.886	0.900	0.891	0.886	0.966	0.973	0.970
M6	25.87	18.09	19.20	18.18	16.64	11.24	12.68	11.30	0.718	0.858	0.841	0.856	0.899	0.960	0.953	0.959
M7	22.28	23.92	24.01	26.42	14.38	15.05	15.40	15.58	0.786	0.754	0.751	0.704	0.932	0.918	0.918	0.892
M8	17.27	14.99	16.58	13.55	10.98	8.93	10.25	8.00	0.872	0.899	0.876	0.918	0.958	0.971	0.963	0.976
M9	31.65	30.85	30.69	30.35	17.38	16.19	15.71	16.16	0.563	0.585	0.589	0.598	0.835	0.850	0.852	0.856
M10	26.05	22.36	22.38	20.75	14.34	9.89	9.30	8.36	0.692	0.770	0.769	0.801	0.891	0.930	0.930	0.942
M11	14.65	12.69	14.00	13.50	9.26	6.57	8.50	7.96	0.907	0.930	0.915	0.920	0.974	0.982	0.977	0.979
M12	13.02	12.12	10.79	9.74	7.52	7.03	5.87	5.27	0.923	0.934	0.947	0.957	0.979	0.981	0.986	0.988
M13	10.45	9.50	7.85	8.34	6.68	4.74	4.14	4.19	0.950	0.958	0.972	0.968	0.987	0.989	0.993	0.992
M14*	10.60	7.49	7.81	7.68	6.03	3.34	3.35	3.26	0.948	0.974	0.972	0.973	0.986	0.993	0.993	0.993

* Indicates the best input combination

particle could be selected as the optimum solution candidate [38]. Empirical observations showed good performance of PSO in optimization [39]. Thus, it has been broadly utilized in complex nonlinear optimization issues [40], [41]. The training process in PSO is started by definition of the initial particle swarm, $P(k)$, so in hyperspace, the position of each particle $(x_{is}(k))$ $(P_i \in P(k))$, is $k = 0$ [42]. Next, the fitness function (F) is assessed for all particle by the position of each particle $(x_i(k))$.

$$if\ F(x_i(k)) < pbest_i \quad then \quad \begin{cases} pbest_i = F(x_i(k)) \\ x_{pbest} = x_i(k) \end{cases} \tag{1}$$

where *pbest* is the best position achieved by particle *i* known as personal best.

The foremost particle efficiency of each individual is then appraised in the following form:

$$if\ F(x_i(k)) < gbest_i \quad then \quad \begin{cases} gbest_i = F(x_i(k)) \\ x_{gbest} = x_i(k) \end{cases} \tag{2}$$

where *gbest*is the global best; the best position obtained by all population.

Next, the velocity vector of each individual is altered as follows:

$$v_i(k) = wv_i(k-1) + r_1C_1(x_{pbest_i} - x_i(k)) + r_2C_2(x_{gbest_i} - x_i(k)) \tag{3}$$

where *r* is selected randomly through training, *C1* and *C2* are two user-defined constants and w is known as weight parameter. The best result can be accomplished when the sum of these two parameters is not more than 4 [42].

Precise determination of the user-defined parameters results an adjustment between the global and local swarm performance, which diminishes the iteration number. The weight parameter (w) is computed in the following form [43]:

$$w = w_{max} - \frac{w_{max} - w_{min}}{iter_{max}}.iter \tag{4}$$

where w_{min} and w_{max} are the initial and final weights, respectively; $iter_{max}$ represents maximum iteration and *iter* the iteration number.

Finally, every particle is transformed to its new position as follows:

$$x_i(k) = x_i(k-1) + v_i(k) \tag{5}$$

C. GENETIC ALGORITHM (GA)

The GA is an evolutionary population-based stochastic optimization technique that has been effectively utilized for solving different optimization issues. GA is proficient in solving nonlinear, stochastic and non-differentiable problems which cannot solve well using gradient-based methods [44]. In conventional optimization approaches, each point is produced utilizing deterministic calculations in each epoch and point sequence in order to achieve the optimum solution. On the other hand, the population points for each epoch are produced haphazardly in GA and the most excellent population have the best solution [45].

Optimization procedure using GA consists of three major steps. First, an initial population of m^{th} individual is randomly created which is considered as the first generation. Next, the performance of each of the m^{th} individual is evaluated based on fitness function value. Finally, offspring as a novel generation is produced using fittest individual of the prior generation. The optimization process is repeated until the optimum solution is achieved.

TABLE 4. Statistical performance of ANFIS, ANFIS-DE, ANFIS-GA and ANFIS-PSO models for different input combinations estimated using RMSE, MAE, R^2 and WI during testing phase.

	RMSE (m^3/s)				MAE (m^3/s)				R^2				WI			
	ANFIS	ANFIS-DE	ANFIS-GA	ANFIS-PSO	ANFIS	ANFIS-DE	ANFIS-GA	ANFIS-PSO	ANFIS	ANFIS-DE	ANFIS-GA	ANFIS-PSO	ANFIS	ANFIS-DE	ANFIS-GA	ANFIS-PSO
M1	33.03	32.97	31.75	31.61	23.67	24.30	21.83	23.03	0.536	0.939	0.726	0.825	0.829	0.827	0.863	0.859
M2	23.22	22.17	21.87	18.05	15.83	15.91	14.62	11.01	0.775	0.950	0.975	0.945	0.936	0.941	0.943	0.963
M3	23.12	17.60	16.88	16.64	15.72	10.87	10.33	10.36	0.779	0.912	0.955	0.974	0.936	0.941	0.943	0.963
M4	23.21	18.75	21.00	18.47	14.84	11.56	13.83	10.69	0.791	0.936	0.956	0.953	0.951	0.968	0.959	0.969
M5	23.57	23.55	18.79	22.53	13.92	15.09	11.54	12.35	0.798	0.864	0.938	0.855	0.948	0.945	0.967	0.948
M6	23.42	17.68	20.82	18.78	15.80	11.11	14.02	12.41	0.775	0.899	0.943	0.956	0.936	0.941	0.943	0.963
M7	21.11	21.26	20.94	22.24	12.25	11.50	11.88	13.10	0.824	0.983	0.985	0.967	0.959	0.959	0.960	0.955
M8	20.89	15.49	17.47	15.48	11.08	7.67	9.47	6.80	0.847	0.966	0.981	0.970	0.959	0.978	0.972	0.978
M9	23.94	22.90	22.78	20.92	14.85	13.68	13.62	12.53	0.773	0.987	0.995	0.981	0.945	0.949	0.950	0.958
M10	19.63	12.12	10.74	9.81	12.79	6.47	5.76	4.72	0.858	0.926	0.981	0.989	0.963	0.986	0.989	0.991
M11	14.32	11.16	13.32	11.71	8.01	5.49	7.64	6.48	0.919	0.980	0.979	0.993	0.982	0.989	0.984	0.988
M12	13.62	12.48	9.28	7.59	7.72	7.51	4.71	3.82	0.932	0.991	0.984	0.997	0.983	0.986	0.992	0.995
M13	12.22	11.02	10.16	5.87	5.97	3.55	3.85	2.49	0.944	0.985	0.991	0.989	0.987	0.989	0.991	0.997
M14*	10.52	8.42	7.90	7.96	3.94	2.33	2.31	2.34	0.958	0.993	0.999	0.998	0.990	0.994	0.994	0.994

* Indicates the best input combination

TABLE 5. Relative error in forecasting of ANFIS, ANFIS-DE, ANFIS-GA and ANFIS-PSO models for different input combination during model testing.

Input combinations	ANFIS	ANFIS-DE	ANFIS-GA	ANFIS-PSO
M1	24.54	19.65	25.99	28.69
M2	19.09	18.65	14.42	21.70
M3	14.46	20.29	18.70	25.68
M4	31.15	41.68	54.20	44.38
M5	30.80	32.27	10.81	6.40
M6	20.67	26.73	25.11	26.96
M7	27.19	24.44	20.74	23.58
M8	89.68	73.34	74.79	77.23
M9	38.77	42.99	46.30	40.54
M10	19.41	16.64	13.53	14.08
M11	23.75	16.56	13.29	13.14
M12	21.52	11.45	5.86	7.89
M13	7.76	10.44	19.47	16.67
M14	9.26	11.17	13.24	11.33

Offspring generation process comprises three essential steps: crossover, mutation and reproduction. In GA, an individual is represented as gene sequence known as chromosomes. The crossover and mutation are employed for reproduction. In crossover, the genes related to parent chromosome are altered, while in mutation genes in parent chromosome are randomly modified. Both of these operators have significant impact on optimization result. Defined operators in GA hop into obscure ranges within the look space (mutation) and offer assistance in finding new solution space (crossover) [46].

The evolutionary process in GA proceeds for different generations until an end condition is satisfied. The best gene is chosen based on the fitness function values and is reported as the optimum solution of the problem.

D. DIFFERENTIAL OPTIMIZATION

Differential Evolution (DE) is an evolutionary population-based optimization algorithm [47]. Use of differential mutation makes the DE different from other evolutionary-based algorithms. In DE, fixed vector numbers are created randomly within n-dimensional space. To discover the different search spaces in order to minimize fitness function, an evolutionary process over time is required. To generate mutation factor (μ), a mutation function ($F : I^{\mu} \rightarrow I^{\mu}$) is defined in the following form:

$$\overrightarrow{v_i} = \overrightarrow{a_{r1}} + F\left(\overrightarrow{a_{r2}} - \overrightarrow{a_{r3}}\right) \quad i = 1, 2, \ldots, \mu \tag{6}$$

where $r_1, r_2, r_3 \in [1, 2, \ldots, \mu]$ are selected randomly, a_i is trial vector, F is the mutation factor and μ is the population size. The mutation factor (F) is a constant positive value in the range of [0 2]. Considering the larger values of population size (μ), mutation factor (F) tends to enhance the global search capacity of DE algorithm by discovering new search space.

The vectors ($\overrightarrow{v_i} = [\overrightarrow{v_{1i}}, \overrightarrow{v_{2i}}, \ldots\ldots, \overrightarrow{v_{di}}]$ are mutated using crossover operator ($CR : I^{\mu} \rightarrow I^{\mu}$) in DE to generate trial vectors as follows:

$$a'_{ji} = \begin{cases} v_{ji} & if \ \ (randb\,(j) \leq CR) \ \ or \ j = rnbr\,(i) \\ a_{ji} & if \ \ (randb\,(j) \leq CR) \ \ or \ j \neq rnbr\,(i) \end{cases} \quad j = 1, 2, \ldots, 2 \quad i = 1, 2, \ldots, d \tag{7}$$

where $rnbr\,(i) \in 1, 2, \ldots, d)$ is an index for random selection, CR is the crossover operator, $randb\,(j)$ denotes randomized producer assessment in the range of [0, 1]. The CR is employed to enhance the individuals' variety in populations. Similar to mutated vectors, large values of CR results in enhancement in offspring vectors. Consequently, the convergence speed of the DE algorithm is augmented.

If cases $CR = 0$, children and parents' vectors differ by only one variable (Eq. 7). The costliest fitness function is selected using selection operator to generate trial vector for next generation.

$$\begin{aligned} &if\ \Phi(\overrightarrow{a_i'}\ (g) < \Phi\left(\overrightarrow{a_i}\ (g)\right), \quad then\ \overrightarrow{a_i}\ (g+1) = \overrightarrow{a_i'}\ (g) \\ &else\ \overrightarrow{a_i}\ (g+1) = \overrightarrow{a_i}\ (g+1) = \overrightarrow{a_i}\ (g) \end{aligned} \tag{8}$$

where g is the current generation.

E. MODELS DEVELOPMENT

Fourteen different combinations of antecedent streamflow values were considered for the selection of best input combination for the development of forecasting models. Usually, most recent antecedent values are more correlated with the target streamflow [11], [12]. Therefore, consecutive two antecedent values, $t-1$ and $t-2$ were considered as possible input. Besides, 3-, 6- and 12-month antecedent values were tested as possible input considering the seasonal variability due to two monsoons and annual variability of streamflow. Indeed, this was determined based on the statistical procedure commonly used for time series forecasting such as autocorrelation function (ACF) as presented in Figure 3. The fourteen input combinations of these five antecedent values are given in Table 1. All the 14 input combinations (M1 to M14) were used for the development of ANFIS and hybrid ANFIS (ANFIS-DE, ANFIS-GA, and ANFIS-PSO) model. The optimum values of the DE, GA, and PSO algorithms are given in Table 2. The values of fixed parameters of ANFIS model were considered as follows: the initial step size is 0.001, step size decrease is 0.009, step size increase is 1.001 and the number of the MF for each input is 6.

F. PERFORMANCE SKILL INDICATORS

To examine the prediction capability of the developed models, several statistical indicators were used which includes mean absolute error (MAE), root mean square error (RMSE), coefficient of determination (R^2) and Willmott's Index *(WI)* [48]–[50]. Besides, the predictive capability of the models was examined using relative error (RE) [51], [52]. The uncertainty in prediction of streamflow by different models was also assessed for fair comparison of model performance. For this purpose, the difference between predicted and target values were first calculated to estimate the prediction error (PE):

$$e_j = P_j - T_j \tag{9}$$

The standard deviation (STD) and mean (MPE) of PE were calculated as:

$$S_e = \sqrt{\sum_{j=1}^{n} \frac{\left(e_j - \bar{e}\right)^2}{n-1}} \quad \text{and} \quad \bar{e} = \sum_{j=1}^{n} e_j \tag{10}$$

A positive (or negative) value of MPE illustrates the overestimation (or underestimation) by the prediction models. Using Wilson score without continuity correction, a confidence band was defined around the predict error values for 95% confidence bound as $\pm 1.96 S_e$ for the estimation of uncertainty in prediction [53].

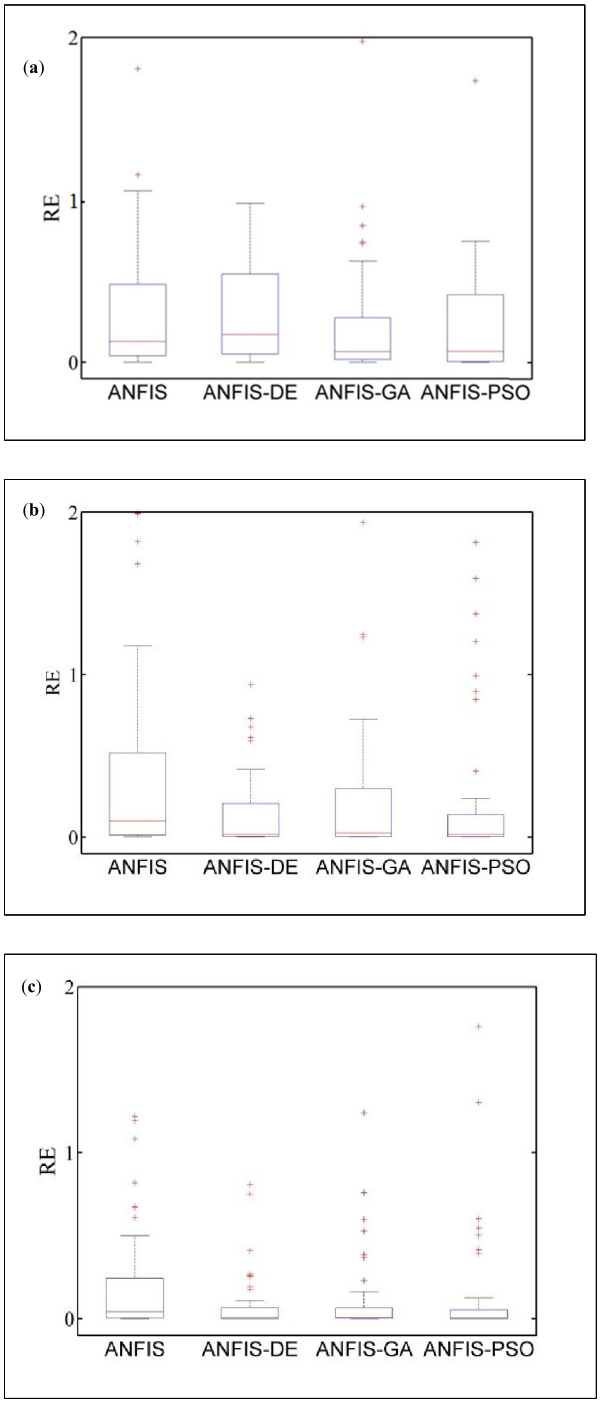

FIGURE 4. Box plots showing the relative errors in streamflow prediction of hybrid and classical ANFIS models for input structures (a) M12, (b) M13, and (c) M14. The symbol '+' indicates outliers in data.

IV. MODELS IMPLEMENTATION AND ANALYSIS

The performance of the models during training for different input combinations (Table 1) are presented in Table 3. The table shows that model 14 produced the highest level of accuracy in terms of RMSE (7.5 to 10.6 m^3/s) and MAE

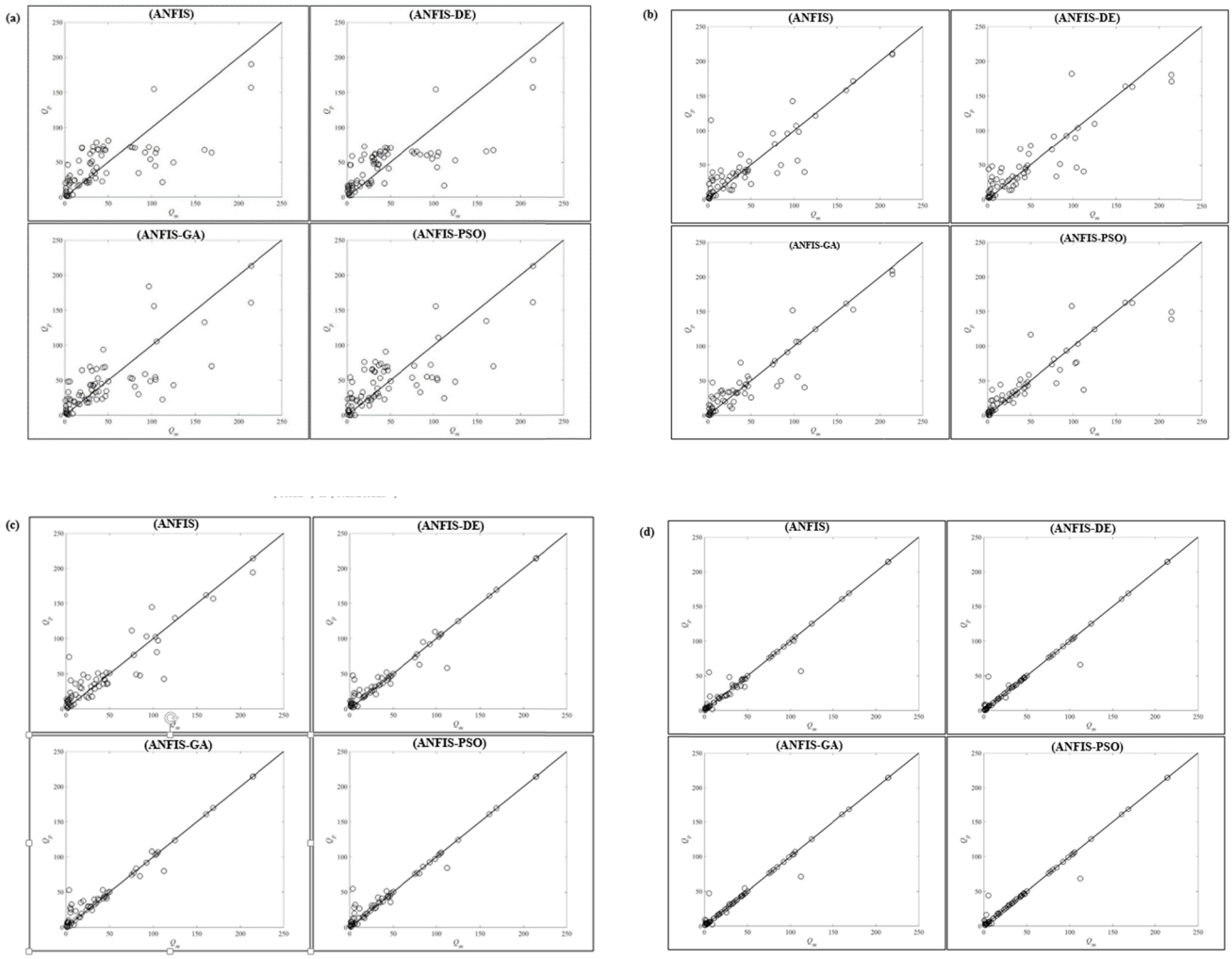

FIGURE 5. The measured (Q_m) and predicted (Q_p) streamflow for (a) Model-M1, (b) Model-M5, (c) Model-M10, and (d) Model-M14. The solid black line represents the line of agreement.

(3.26 to 6.03 m^3/s). The forecasting ability the models, particularly for hybrid-ANFIS models improved significantly with more inputs (M14). It is interesting to note that the RMSE and MAE values were consistently decreased from M9 to M14 for all the predictive models. In general, the hybrid ANFIS models showed lowest RMSE (7.5 – 7.8 m^3/s) and MAE (3.3-3.4 m^3/s) for M14. High accuracy for larger input combinations was also supported by high R^2 and *WI* values, particularly for M14.

The performance of the models during testing phase is presented in Table 4. Considering $t-1$ alone and with another single antecedent values (M1 to M5), the lowest RMSE and MAE were obtained for M3 which considered $t-3$ as an additional input with $t-1$. Comparison of three input models (M6 to M8) where two inputs ($t-1$ and $t-2$) were common showed higher impact of $t-12$ in performance of all the hybrid ANFIS models compared to inputs $t-3$ and $t-6$. The only difference of M9 and M10 from M6 was the use of $t-6$ and $t-12$ instead of $t-2$. The results revealed that the use of $t-2$ instead of $t-12$ improved the accuracy of ANFIS-GA and ANFIS-DE models by 10% in term of RMSE. The MAE, R^2 and *WI* values for M10 (for all hybrid ANFIS models) were found to improve compared to M6. Considering $t-3$ instead of $t-2$ in addition to $t-1$ and $t-12$ (M10 and M8, respectively) caused significant increase in RMSE, MAE and WI for all the hybrid ANFIS models. This indicates that $t-3$ as a seasonal lag is more important than $t-2$.

Generally, a decreasing trend in RMSE and MAE was observed from M1 to M14 for all the hybrid models. Predicted streamflow values were found more accurate for 4-input combination and it reached to the highest level of accuracy for 5-input combination (M14).

In general, M14 showed the lowest RMSE for ANFIS (10.5), ANFIS-DE (8.4) and ANFIS-GA (7.9), whereas the lowest RMSE (5.87 m^3/s) for ANFIS-PSO was obtained for M13. The lowest MAE and the highest R^2 and WI were also found consistently associated with M14 (MAE = 2.31 m^3/s; $R^2 = 0.999$; WI = 0.994). The results indicate that all of seasonal lags (i.e. $t-3$, $t-6$ and $t-12$) have significant effect on prediction of streamflow.

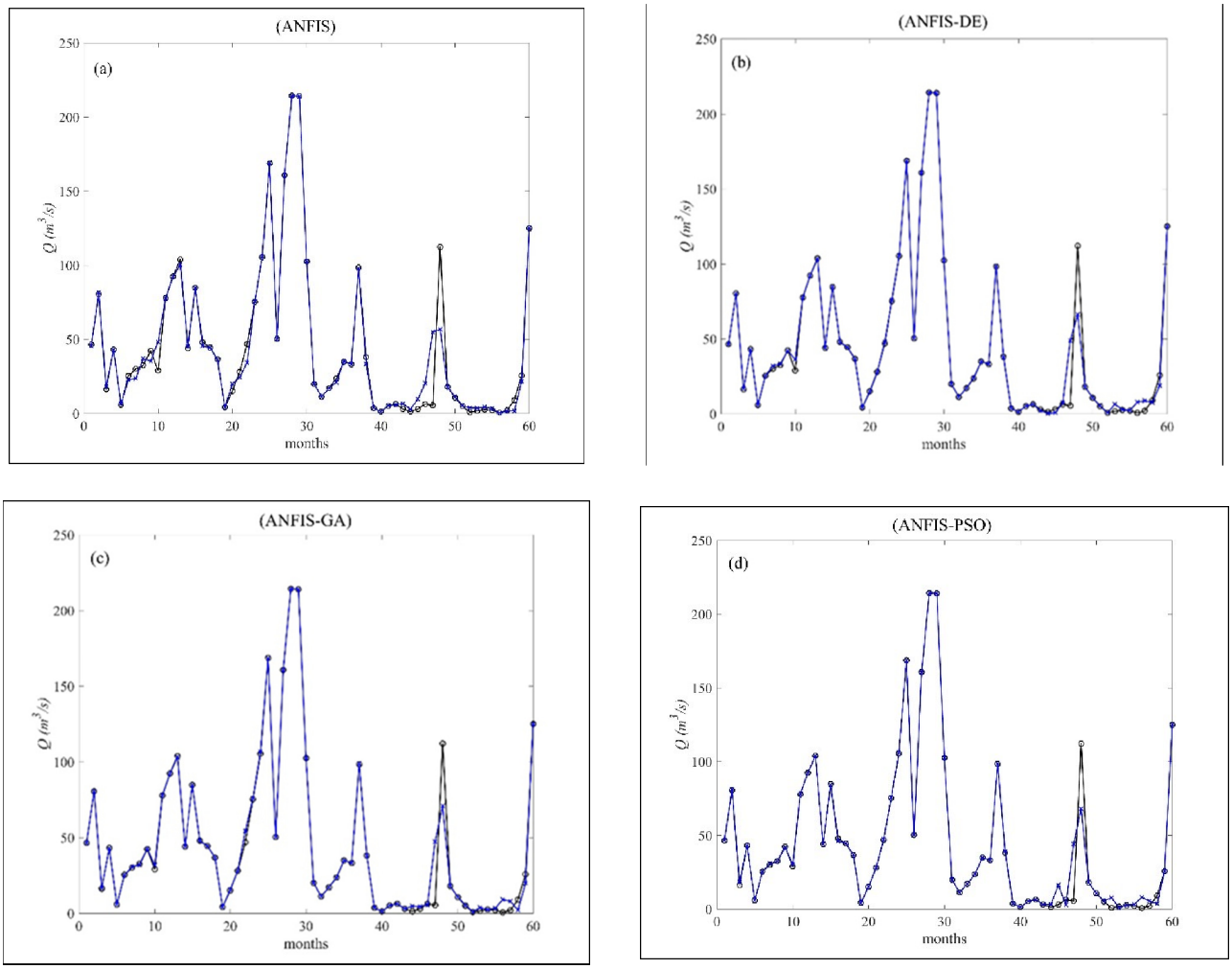

FIGURE 6. Time series plots of measured (Q_m) and predicted (Q_p) streamflow for input structure M14 using (a) ANFIS, (b), ANFIS-DE, (c) ANFIS-GA and (d) ANFIS-PSO models. The black and blue lines represent the measured and predicted streamflow, respectively.

To assert the results obtained above, the relative errors in model predictions using different input combinations were estimated and presented in Table 5. The range of relative errors was found between 5.86 and 89.68%. Interestingly, the maximum relative error *(RE)* was found incidentally for structure M8 for all the models, while the minimum *RE* was found to vary. The lowest RE was found for ANFIS-GA for M12 (5.86%), whereas M5 (6.4%) and M13 (10.44%) showed the lowest RE for ANFIS-PSO and ANFIS-DE, respectively. The classical ANFIS model showed the lowest RE for the input combination (M13). Although M14 not showed a remarkable improvement in term of RE for any of the predictive models, in general a low percentage of RE (below 15%) was observed for all the models. Taking into account of the model performance for different input combinations, M14 was found as the best followed by M13 and M12.

Figure 4 shows the box plots of RE for the best three input combinations, M12 to M14. A rather consistent behavior was observed for the three hybrid ANFIS models for structure M12. The box height was found smaller for ANFIS-GA which indicates ANFIS-GA as the best hybrid model for M12. Much smaller range of RE was observed for M13 compared to M12 particularly for ANFIS-DE and ANFIS-PSO. The boxplot of RE for ANFIS was found the tallest among the four, which indicates better performance of hybrid ANFIS models compared to classical ANFIS. The M14 produced the smallest range of RE compared to other input structures. The smallest ranges of RE were found for hybrid ANFIS models when the input structure was M14. Furthermore, the median values of RE of different hybrid ANFIS models were found very close to 0, suggesting a high level of accuracy of the models.

The results indicate that models with a higher number of inputs have higher prediction accuracy. The results are in agreement with the hybrid model forecasts obtained by [54], [55], where a 3-input model was found to provide better accuracy than a 1- or 2-input model. The results also indicate that incorporation of longer antecedent data improves the prediction capability as the model is able to capture the seasonal pattern and existing trend in time series more accurately. The rainfall of Malaysia is highly variable due to two

TABLE 6. Uncertainty in prediction of hybrid and classical ANFIS models.

Model	MPE	STD of PE	WUB	95% PEI
ANFIS	1.202	1.355	±0.3185	(0.884 1.521)
ANFIS-DE	0.759	1.077	±0.253	(0.506 1.012)
ANFIS-GA	0.782	1.088	±0.2555	(0.526 1.037)
ANFIS-PSO	0.647	0.922	±0.217	(0.430 0.864)

monsoon seasons, southwest monsoon (May–September) and northeast monsoon (November–February). Incorporation of longer antecedent data helps to capture the low, medium and high flow conditions due to seasonal changes and thus more information of the fluctuation of streamflow. The models were able to capture the nonlinear streamflow behavior when twelfth antecedent value was used [56]. The results clearly indicate M14 as the best input combination and therefore, the ability of the models in forecasting streamflow was tested only for M14.

Scatterplots were prepared for four input combinations (M1, M5, M10, and M14). The figures demonstrate the variance between the measured and forecasted streamflow. M14 for all the applied hybrid models was found to forecast both low and high flows satisfactorily. Most of the data were found on the line of agreement (Figure 5). However, some over- and under- estimation were noticed for ANFIS and ANFIS-DE. Lower number of paired points was observed for ANFIS-GA and ANFIS-PSO, respectively.

It is rather obvious that hybrid ANFIS models have better prediction capability than classical ANFIS model as shown in Figure 5. Most of the streamflow values were estimated with highest accuracy, for both low and high flows. However, the accurate prediction was not necessarily certain for all the observations, as evident for months no 41 to 48 where low flows were overestimated and high flows were underestimated. This is most probably due to the inability of the predictive models to capture the sudden increment in the river flow due to monsoon heavy rainfall. The high intensity of tropical rainfall events where it could be up to 600 mm, particularly in December cause immediate increase of streamflow [56]. The models however eventually able to capture the dynamicity of the discharge pattern, where the consequential sudden high flow (at sample no 60) was accurately predicted by the models. Focusing on the 48th month, although the predicted peak was overly underestimated, the hybrid ANFIS models performed better than the non-hybrid ANFIS.

It is worth to highlight that although appropriate time lags (having the highest autocorrelation) and longer time lags increase the accuracy, the improvement is not comparable when an intelligent pre-processing approach is used. This study shows that DE and PSO give a relatively highest accuracy in streamflow forecasting compared to GA.

TABLE 7. Optimum value of the gaussion membership function (MF) related to the best model (ANFIS-PSO).

Input	MF	Sigma	C
t-1	MF 1	33.5095	116.5279
	MF 2	33.3558	114.9862
	MF 3	33.2348	113.7421
	MF 4	32.5018	104.5094
	MF 5	33.1616	112.9575
	MF 6	33.373	115.1547
t-2	MF 1	33.4076	115.5269
	MF 2	33.2925	114.3333
	MF 3	33.2005	113.3636
	MF 4	32.605	105.9839
	MF 5	33.142	112.7481
	MF 6	33.3043	114.4643
t-3	MF 1	33.2061	113.4811
	MF 2	33.1601	112.9582
	MF 3	33.1231	112.5212
	MF 4	32.8237	108.8146
	MF 5	33.0986	112.2361
	MF 6	33.1649	113.0166
t-6	MF 1	32.8152	108.8146
	MF 2	32.9211	109.895
	MF 3	33.0108	110.7649
	MF 4	33.7392	117.0881
	MF 5	33.0691	111.3116
	MF 6	32.9097	109.7767
t-12	MF 1	33.4881	116.3831
	MF 2	33.3591	115.0267
	MF 3	33.2567	113.9223
	MF 4	32.6003	105.4616
	MF 5	33.191	113.221
	MF 6	33.3728	115.1762

The forecasted streamflow during model testing was used for uncertainty analysis. The results of uncertainty analysis for four ANFIS-based models are presented in Table 6. The table shows STD, MPE and 95% prediction error interval (PEI) of streamflow as well as the width of uncertainty bound (WUB). The results indicate that all the hybrid ANFIS models outperformed the classical ANFIS model. The MPE for ANFIS was 1.202 compared to 0.759, 0.782, and 0.647 (m^3/s) for ANFIS-DE, ANFIS-GA and ANFIS-PSO, respectively. The ANFIS-PSO showed the lowest and the ANFIS-GA showed the highest MPE among the hybrid

models. The uncertainty bound for hybrid models were in the range of ±0.22 to ±0.26, while it was found ±0.3185 for the classical ANFIS. The highest 95%PEI was observed for classical ANFIS, while the lowest MPE and WUB were observed for ANFIS-PSO. The optimum value related to the best model is presented in Table 7.

The most crucial characteristics of time series forecasting model is its capability to capture the pattern exist in the series and generalize the captured pattern outside the domain of calibration data. The performance of a data driven models to generalize the captured pattern depends on the complexity of the time series to be forecasted. It is not possible to decide which model is best for forecasting a time series without comparing the performance of different models. Even when a data driven method is found suitable for forecasting a time series, its performance largely depends on the tuning of its hyper parameters. Proper tuning of parameters allows better mapping of input-output relationship. Besides, when the time series forecasting is only based on historical data of the same series, selection of optimum combination of antecedent time lag data as input is important as inappropriate input can propagate error to output and deteriorate prediction accuracy. Therefore, performance of different tuning algorithms was assessed in this study for different combinations of inputs in order to find the most appropriate model in term of both tuning algorithm and input combination. The present study revealed that ANFIS model is capable to capture the pattern of streamflow time series and generalize the pattern for forecasting streamflow with unknown data when its parameters were tuned with PSO and five antecedent data including three most recent data and the seasonal and annual lag data were used as input. Though ANFIS-PSO with five inputs was found as the best model for forecasting monthly streamflow in tropical environment, it cannot be guaranteed that same model will perform best in other environment, even for other river in tropical region. The framework proposed in this study can be used for the selection of the state-of-art optimization method for the tuning of model parameter and selection of best input combination for the selection of most accurate forecasting model for any other study area.

V. CONCLUSION

Three different evolutionary algorithms namely, GA, DE, and PSO were integrated with ANFIS for forecasting highly stochastic monthly streamflow of a tropic river. Fourteen different combinations of antecedent streamflow values were considered for the selection of best input combination for the development of the forecasting models. The results indicated that incorporation of longer antecedent data improves the prediction capability as the model is able to capture the seasonal pattern and the existing trend in time series more accurately. The best performance was obtained for the model with 5 input variables ($t-1, t-2, t-3, t-6, t-12$), with a 68% prediction improvement than the model with 1 input variable ($t-1$). Comparison of the performance of the evolutionary hybrid ANFIS models with the classical ANFIS model revealed the ability of evolutionary algorithms in the optimization of ANFIS membership function in order to minimize the prediction error. Comparison of evolutionary optimization techniques indicated the higher capability of PSO in optimization of ANFIS membership functions compared to GA and DE. ANFIS-PSO model provided better prediction than non-hybrid ANFIS by 25%, slightly higher than ANFIS-GA and ANFIS-DE (24% and 20%, respectively). The uncertainty analysis revealed the lowest width of uncertainty band for ANFIS-PSO than the other hybrid methods and classical ANFIS. Therefore, the ANFIS-PSO model can be used for reliable forecasting of highly stochastic river flow in tropical environment.

DATA AVAILABILITY

Hydrological data obtained from the Department of Irrigation and Drainage (DID), Malaysia.

ACKNOWLEDGMENT

Authors would like to acknowledge their gratitude to the Department of Irrigation and Drainage (DID), Malaysia, for providing streamflow data of Pahang River. Also, authors appreciate the three reviewers and the Editors whose comments have improved the overall quality of this research paper.

CONFLICTS OF INTEREST

The authors declare no conflict of interest.

REFERENCES

[1] C.-F. Yeh, J. Wang, H.-F. Yeh, and C.-H. Lee, "Spatial and temporal streamflow trends in northern taiwan," *Water*, vol. 7, no. 2, pp. 634–651, 2015.
[2] L. Sun, I. Nistor, and O. Seidou, "Streamflow data assimilation in SWAT model using extended Kalman filter," *J. Hydrol.*, vol. 531, pp. 671–684, Dec. 2015.
[3] Y. Liu, J. Guo, H. Sun, W. Zhang, Y. Wang, and J. Zhou, "Multiobjective optimal algorithm for automatic calibration of daily streamflow forecasting model," *Math. Problems Eng.*, vol. 2016, Jul. 2016, Art. no. 8215308.
[4] L. E. Besaw, D. M. Rizzo, P. R. Bierman, and W. R. Hackett, "Advances in ungauged streamflow prediction using artificial neural networks," *J. Hydrol.*, vol. 386, pp. 27–37, May 2010.
[5] C. L. Wu, K. W. Chau, and Y. S. Li, "Predicting monthly streamflow using data-driven models coupled with data-preprocessing techniques," *Water Resour. Res.*, vol. 45, no. 8, pp. 1–23, 2009.
[6] R. Maity, P. P. Bhagwat, and A. Bhatnagar, "Potential of support vector regression for prediction of monthly streamflow using endogenous property," *Hydrol. Process.*, vol. 24, no. 7, pp. 917–923, 2010.
[7] Z. A. Al-Sudani, S. Q. Salih, A. Sharafati, and Z. M. Yaseen, "Development of multivariate adaptive regression spline integrated with differential evolution model for streamflow simulation," *J. Hydrol.*, vol. 573, pp. 1–12, Jun. 2019.
[8] L. Diop, A. Bodian, K. Djaman, Z. M. Yaseen, R. C. Deo, A. El-Shafie, and L. C. Brown, "The influence of climatic inputs on stream-flow pattern forecasting: Case study of upper senegal river," *Environ. Earth Sci.*, vol. 77, no. 5, p. 182, 2018.
[9] J. E. Shortridge, S. D. Guikema, and B. F. Zaitchik, "Machine learning methods for empirical streamflow simulation: A comparison of model accuracy, interpretability, and uncertainty in seasonal watersheds," *Hydrol. Earth Syst. Sci.*, vol. 20, no. 7, pp. 2611–2628, 2016.
[10] F. Fahimi, Z. M. Yaseen, and A. El-Shafie, "Application of soft computing based hybrid models in hydrological variables modeling: A comprehensive review," *Theor. Appl. Climatol.*, vol. 128, pp. 875–903, May 2016.
[11] M. A. Ghorbani, R. Khatibi, V. Karimi, Z. M. Yaseen, and M. Zounemat-Kermani, "Learning from multiple models using artificial intelligence to improve model prediction accuracies: Application to river flows," *Water Resour. Manage.*, vol. 32, no. 13, pp. 4201–4215, 2018.

[12] Z. M. Yaseen, A. El-shafie, O. Jaafar, H. A. Afan, and K. N. Sayl, "Artificial intelligence based models for stream-flow forecasting: 2000–2015," *J. Hydrol.*, vol. 530, pp. 829–844, Nov. 2015.
[13] Z. M. Yaseen, S. O. Sulaiman, R. C. Deo, and K.-W. Chau, "An enhanced extreme learning machine model for river flow forecasting: State-of-the-art, practical applications in water resource engineering area and future research direction," *J. Hydrol.*, vol. 569, pp. 387–408, Feb. 2019.
[14] R. J. Abrahart, F. Anctil, P. Coulibaly, C. W. Dawson, N. J. Mount, L. M. See, A. Y. Shamseldin, D. P. Solomatine, E. Toth, and R. L. Wilby, "Two decades of anarchy? Emerging themes and outstanding challenges for neural network river forecasting," *Prog. Phys. Geogr., Earth Environ.*, vol. 36, no. 4, pp. 480–513, 2012.
[15] W. Wang, P. H. A. J. M. Van Gelder, J. K. Vrijling, and J. Ma, "Forecasting daily streamflow using hybrid ANN models," *J. Hydrol.*, vol. 324, nos. 1–4, pp. 383–399, 2006.
[16] S. Isik, L. Kalin, J. E. Schoonover, P. Srivastava, and B. G. Lockaby, "Modeling effects of changing land use/cover on daily streamflow: An artificial neural network and curve number based hybrid approach," *J. Hydrol.*, vol. 485, pp. 103–112, Apr. 2013.
[17] M. Kothari and K. D. Gharde, "Application of ANN and fuzzy logic algorithms for streamflow modelling of Savitri catchment," *J. Earth Syst. Sci.*, vol. 124, no. 5, pp. 933–943, 2015.
[18] M. Demirci and A. Baltaci, "Prediction of suspended sediment in river using fuzzy logic and multilinear regression approaches," *Neural Comput. Appl.*, vol. 23, pp. 145–151, Dec. 2013.
[19] G. Tayfur and L. Brocca, "Fuzzy logic for rainfall-runoff modelling considering soil moisture," *Water Resour. Manage.*, vol. 29, no. 10, pp. 3519–3533, 2015.
[20] Z. M. Yaseen, M. I. Ghareb, I. Ebtehaj, H. Bonakdari, R. Siddique, S. Heddam, A. A. Yusif, and R. Deo, "Rainfall pattern forecasting using novel hybrid intelligent model based ANFIS-FFA," *Water Resour. Manage.*, vol. 32, no. 1, pp. 105–122, 2018.
[21] O. Kisi and Z. M. Yaseen, "The potential of hybrid evolutionary fuzzy intelligence model for suspended sediment concentration prediction," *Catena*, vol. 174, pp. 11–23, May 2019.
[22] V. S. Ghomsheh, M. A. Shoorehdeli, and M. Teshnehlab, "Training ANFIS structure with modified PSO algorithm," in *Proc. Medit. Conf. Control Automat.*, 2007, pp. 1–6.
[23] Z. M. Yaseen, I. Ebtehaj, H. Bonakdari, R. C. Deo, A. D. Mehr, W. H. M. W. Mohtar, L. Diop, A. El-Shafie, and V. P. Singh, "Novel approach for streamflow forecasting using a hybrid ANFIS-FFA model," *J. Hydrol.*, vol. 554, pp. 263–276, Nov. 2017.
[24] H. R. Maier *et al.*, "Evolutionary algorithms and other metaheuristics in water resources: Current status, research challenges and future directions," *Environ. Model. Softw.*, vol. 62, pp. 271–299, Dec. 2014.
[25] A. P. Piotrowski and J. J. Napiorkowski, "Optimizing neural networks for river flow forecasting—Evolutionary computation methods versus the Levenberg–Marquardt approach," *J. Hydrol.*, vol. 407, nos. 1–4, pp. 12–27, 2011.
[26] M. A. Shoorehdeli, M. Teshnehlab, and A. K. Sedigh, "A novel training algorithm in ANFIS structure," in *Proc. Amer. Control Conf.*, 2006, p. 6.
[27] J. T. Lalis, B. D. Gerardo, and Y. Byun, "An adaptive stopping criterion for backpropagation learning in feedforward neural network," *Int. J. Multimedia Ubiquitous Eng.*, vol. 9, no. 8, pp. 149–156, 2014.
[28] Y. W. Chen, L. C. Chang, C. W. Huang, and H. J. Chu, "Applying genetic algorithm and neural network to the conjunctive use of surface and subsurface water," *Water Resour. Manage.*, vol. 27, no. 14, pp. 4731–4757, 2013.
[29] E. Tapoglou, I. C. Trichakis, Z. Dokou, I. K. Nikolos, and G. P. Karatzas, "Groundwater-level forecasting under climate change scenarios using an artificial neural network trained with particle swarm optimization," *Hydrolog. Sci. J.*, vol. 59, no. 6, pp. 1225–1239, 2014.
[30] I. Ebtehaj and H. Bonakdari, "Comparison of genetic algorithm and imperialist competitive algorithms in predicting bed load transport in clean pipe," *Water Sci. Technol.*, vol. 70, no. 10, pp. 1695–1701, 2014.
[31] S. R. Naganna, P. C. Deka, M. A. Ghorbani, S. M. Biazar, N. Al-Ansari, and Z. M. Yaseen, "Dew point temperature estimation: Application of artificial intelligence model integrated with nature-inspired optimization algorithms," *Water*, vol. 11, no. 4, p. 742, 2019.
[32] A. Zimmer, A. Schmidt, A. Ostfeld, and B. Minsker, "Evolutionary algorithm enhancement for model predictive control and real-time decision support," *Environ. Model. Softw.*, vol. 69, pp. 330–341, Jul. 2015.
[33] S. Maroufpoor, E. Maroufpoor, O. Bozorg-Haddad, J. Shiri, and Z. M. Yaseen, "Soil moisture simulation using hybrid artificial intelligent model: Hybridization of adaptive neuro fuzzy inference system with grey wolf optimizer algorithm," *J. Hydrol.*, vol. 575, pp. 544–556, Aug. 2019.
[34] W. Chen, M. Panahi, and H. R. Pourghasemi, "Performance evaluation of GIS-based new ensemble data mining techniques of adaptive neuro-fuzzy inference system (ANFIS) with genetic algorithm (GA), differential evolution (DE), and particle swarm optimization (PSO) for landslide spatial modelling," *Catena*, vol. 157, pp. 310–324, Oct. 2017.
[35] M. B. Gasim, M. E. Toriman, I. Mushrifah, P. Lun, M. K. A. Kamarudin, A. A. A. Nor, M. Mazlin, and M. S. A. Sharifah, "River flow conditions and dynamic state analysis of Pahang river," *Amer. J. Appl. Sci.*, vol. 10, no. 1, pp. 42–57, 2013.
[36] A. Ab Ghani, C. K. Chang, C. S. Leow, and N. A. Zakaria, "Sungai Pahang digital flood mapping: 2007 flood," *Int. J. River Basin Manage.*, vol. 10, no. 2, pp. 139–148, 2012.
[37] J.-S. R. Jang, "ANFIS: Adaptive-network-based fuzzy inference system," *IEEE Trans. Syst., Man, Cybern.*, vol. 23, no. 3, pp. 665–685, May/Jun. 1993.
[38] I. Ebtehaj and H. Bonakdari, "Performance evaluation of adaptive neural fuzzy inference system for sediment transport in sewers," *Water Resour. Manage.*, vol. 28, no. 13, pp. 4765–4779, 2014.
[39] J. Kennedy and R. Eberhart, "A new optimizer using particle swarm theory," in *Proc. 6th Int. Symp. Micro Mach. Hum. Sci.*, 1995, pp. 39–43.
[40] W.-J. Yu, J.-Z. Li, W.-N. Chen, and J. Zhang, "A parallel double-level multiobjective evolutionary algorithm for robust optimization," *Appl. Soft Comput.*, vol. 59, pp. 258–275, Oct. 2017.
[41] W. Srisukkham, L. Zhang, S. C. Neoh, S. Todryk, and C. P. Lim, "Intelligent leukaemia diagnosis with bare-bones PSO based feature optimization," *Appl. Soft Comput.*, vol. 56, pp. 405–419, Jul. 2017.
[42] I. Ebtehaj and H. Bonakdari, "Assessment of evolutionary algorithms in predicting non-deposition sediment transport," *Urban Water J.*, vol. 13, no. 5, pp. 499–510, 2016.
[43] H. Moeeni, H. Bonakdari, and I. Ebtehaj, "Integrated SARIMA with neuro-fuzzy systems and neural networks for monthly inflow prediction," *Water Resour. Manage.*, vol. 31, no. 7, pp. 2141–2156, 2017.
[44] M. Jakubcová, P. Máca, and P. Pech, "Parameter estimation in rainfall-runoff modelling using distributed versions of particle swarm optimization algorithm," *Math. Problems Eng.*, vol. 2015, Aug. 2015, Art. no. 968067.
[45] Y.-H. Chen and F.-J. Chang, "Evolutionary artificial neural networks for hydrological systems forecasting," *J. Hydrol.*, vol. 367, nos. 1–2, pp. 125–137, 2009.
[46] J. H. Holland, "Genetic algorithms," *Sci. Amer.*, vol. 267, no. 1, pp. 66–72, Jul. 1992.
[47] R. Storn and K. Price, "Differential evolution—A simple and efficient heuristic for global optimization over continuous spaces," *J. Global Optim.*, vol. 11, no. 4, pp. 341–359, 1997.
[48] H. Tao, L. Diop, A. Bodian, K. Djaman, P. M. Ndiaye, and Z. M. Yaseen, "Reference evapotranspiration prediction using hybridized fuzzy model with firefly algorithm: Regional case study in Burkina Faso," *Agricult. Water Manage.*, vol. 208, pp. 140–151, Sep. 2018.
[49] T. Chai and R. R. Draxler, "Root mean square error (RMSE) or mean absolute error (MAE)?—Arguments against avoiding RMSE in the literature," *Geosci. Model Develop.*, vol. 7, no. 3, pp. 1247–1250, 2014.
[50] C. J. Willmott, S. M. Robeson, and K. Matsuura, "A refined index of model performance," *Int. J. Climatol.*, vol. 32, no. 13, pp. 2088–2094, 2011.
[51] H. Sanikhani, R. C. Deo, Z. M. Yaseen, O. Eray, and O. Kisi, "Non-tuned data intelligent model for soil temperature estimation: A new approach," *Geoderma*, vol. 330, pp. 52–64, Nov. 2018.
[52] Z. M. Yaseen, M. T. Tran, S. Kim, T. Bakhshpoori, and R. C. Deo, "Shear strength prediction of steel fiber reinforced concrete beam using hybrid intelligence models: A new approach," *Eng. Struct.*, vol. 177, no. April, pp. 244–255, 2018.
[53] I. Ebtehaj, H. Bonakdari, and S. Shamshirband, "Extreme learning machine assessment for estimating sediment transport in open channels," *Eng. Comput.*, vol. 32, no. 4, pp. 691–704, 2016.
[54] H. Badrzadeh, R. Sarukkalige, and A. W. Jayawardena, "Impact of multi-resolution analysis of artificial intelligence models inputs on multi-step ahead river flow forecasting," *J. Hydrol.*, vol. 507, pp. 75–85, 2013.
[55] C. Sudheer, R. Maheswaran, B. K. Panigrahi, and S. Mathur, "A hybrid SVM-PSO model for forecasting monthly streamflow," *Neural Comput. Appl.*, vol. 24, no. 6, pp. 1381–1389, 2013.
[56] N. H. Sulaiman, M. K. A. Kamarudin, M. E. Toriman, H. Juahir, F. M. Ata, A. Azid, N. J. A. Wahab, R. Umar, S. I. Khalit, M. Makhtar, A. Arfan, and U. Sideng, "Relationship of rainfall distribution and water level on major flood 2014 in Pahang River Basin, Malaysia," *EnvironmentAsia*, vol. 10, no. 1, pp. 1–8, 2017.